

Electronic structures of double perovskites $\text{Sr}_2(\text{Fe}_{1-z}\text{Mn}_z)\text{MoO}_6$: Doping-dependent optical studies

J. H. Jung and S.-J. Oh

School of Physics and Center for Strongly Correlated Materials Research, Seoul National University, Seoul 151-747, Korea

M. W. Kim and T. W. Noh

School of Physics and Research Center for Oxide Electronics, Seoul National University, Seoul 151-747, Korea

J.-Y. Kim

Pohang Light Source and Electron Spin Science Center, Pohang University of Science and Technology, Pohang 790-784, Korea

J.-H. Park

Department of Physics and Electron Spin Science Center, Pohang University of Science and Technology, Pohang 790-784, Korea

H.-J. Lin and C. T. Chen

Synchrotron Radiation Research Center, Hsinchu 30077, Taiwan

Y. Moritomo

CIRSE, Nagoya University, Nagoya 464-8603, Japan

(Received 28 January 2002; published 16 September 2002)

We investigated the optical conductivity spectra $\sigma(\omega)$ of double perovskites $\text{Sr}_2(\text{Fe}_{1-z}\text{Mn}_z)\text{MoO}_6$, which show filling controlled metal–insulator transition. Based on systematic analyses of optical conductivity and O 1s x-ray absorption spectroscopy, the electronic structures of both $\text{Sr}_2\text{FeMoO}_6$ and $\text{Sr}_2\text{MnMoO}_6$ near the Fermi level are presented, which turn out to agree with the recent LSDA+U calculation results [H. Wu, Phys. Rev. B **64**, 125126 (2001)]. With the Mo carrier doping (with z decreasing), the in-gap spectral weight is formed, below the gap of $\text{Sr}_2\text{MnMoO}_6$, and finally developed into a Drude peak in $\text{Sr}_2\text{FeMoO}_6$. Due to the possible site disorder, finite energy peaks rather than Drude-like peaks were observed for most of the doping ranges $0.2 \leq z \leq 0.8$. With the ferrimagnetic ordering, we observed redistribution of spectral weight over a wide energy region from 0 to 3 eV. The high energy spectral weight was transferred to the low energy region, similar to the manganites. We discussed possible scenarios relevant to the Fe–Mo hybridization.

DOI: 10.1103/PhysRevB.66.104415

PACS number(s): PACS number; 75.70.Pa, 71.30.+h, 78.20.–e

I. INTRODUCTION

Magnetoresistance phenomena in magnetic oxides have attracted a great deal of attention due to scientific as well as technological importance. The discovery of colossal magnetoresistance in doped manganites has prompted extensive research.¹ However, their low magnetic ordering temperature and high magnetic field requirements have undermined their potential in technological applications. Recently, Kobayashi *et al.*² reported large, low-field, tunneling type magnetoresistance even at room temperature in ordered double perovskites $A_2B'B''O_6$, where A is an alkaline ion, and B' and B'' are transition metals.

Among the ordered double perovskites, $\text{Sr}_2\text{FeMoO}_6$ has been extensively studied.^{3–5} It is known that the FeO_6 and MoO_6 octahedra are alternately ordered in a rock-salt lattice and the angle of the Fe–O–Mo chain is nearly 180° . Magnetization data indicate a ferrimagnetic ordering with a high ordering temperature $T_c \sim 420$ K, in which spins at the $\text{Fe}^{3+}(3d^5)$ and $\text{Mo}^{5+}(4d^1)$ ions are aligned in the opposite direction to each other. A theoretical band calculation predicted that this material is a half-metal, where the Mo t_{2g} down-spin band (hybridized with the Fe t_{2g} down-spin band) crosses the Fermi level, but the up-spin band is separated

by an insulating gap.² Meanwhile, another double perovskite $\text{Sr}_2\text{MnMoO}_6$ with $\text{Mn}^{2+}(3d^5)$ and $\text{Mo}^{6+}(4d^0)$ ions has been known to be either a paramagnetic or antiferromagnetic insulator.⁶ Here, the Mo $4d$ band is fully unoccupied, and antiferromagnetic insulating behavior due to the superexchange interaction has been suggested. Hence, $\text{Sr}_2(\text{Fe},\text{Mn})\text{MoO}_6$ compound is an appropriate candidate for the investigation of the metal–insulator transition caused by the Mo $4d$ band filling without significant changes of the $S = 5/2$ spin background formed with the Fe^{3+} or Mn^{2+} ions.

Optical spectroscopies have been known to be quite useful for investigating electronic structures near the Fermi level and electrodynamic responses related to metal–insulator transitions, as demonstrated in manganites.⁷ Note that both double perovskites and manganites are half-metals and show colossal magnetoresistance. In spite of these similarities, there have been few investigations on the electronic structure of double perovskites.^{8,9} Few spectroscopic investigations have been performed on the electronic structure changes near the ferrimagnetic ordering and metal–insulator transition. In this paper, we report the temperature- and doping-dependent optical conductivity spectra $\sigma(\omega)$ of $\text{Sr}_2(\text{Fe}_{1-z}\text{Mn}_z)\text{MoO}_6$. By combining the results with the O 1s x-ray absorption spectroscopy (XAS) data, we can clarify the electronic struc-

tures of $\text{Sr}_2\text{FeMoO}_6$ and $\text{Sr}_2\text{MnMoO}_6$ in detail. We observe the spectral weight changes of $\sigma(\omega)$ in a wide energy region below 3 eV not only with variation of the doping concentration but also with temperature. We will discuss the spectral weight changes based on the detailed electronic structure and the Mo–Fe hybridization.

II. EXPERIMENTS

A series of $\text{Sr}_2(\text{Fe}_{1-z}\text{Mn}_z)\text{MoO}_6$ ($z=0.0, 0.2, 0.4, 0.6, 0.8,$ and 1.0) single crystals were grown by the floating zone method. X-ray diffraction measurements showed that all the samples were in single-phases, and the ordering of the Fe(Mn) and Mo ions was also confirmed by the corresponding superlattice peaks. Using the Rietveld refinement of the synchrotron x-ray powder pattern, we estimated the ordering of the Fe(Mn) and Mo ions. The ordering of the Fe(Mn) and Mo ions was estimated around 85% in $z=0.0$ and increased with z . For electrical and magnetic properties, we performed dc resistivity and magnetization measurements using the four-probe method and a commercial Superconducting Quantum Interference Device (SQUID) magnetometer, respectively. Details of sample growth and characterization were reported elsewhere.¹⁰

The O 1s XAS measurements, which are well known to probe the electronic structures of the conduction bands,¹¹ were performed at the high-resolution Dragon beamline at Synchrotron Radiation Research Center (SRRC) in Taiwan. The incoming photon resolution was set to ~ 200 meV, and the absorption spectra were recorded in the bulk sensitive fluorescence yield mode with a penetration depth of ~ 1000 Å.

The reflectivity spectra $R(\omega)$ of $\text{Sr}_2(\text{Fe}_{1-z}\text{Mn}_z)\text{MoO}_6$ were measured in the energy region of 5 meV–20 eV. A Fourier transform spectrophotometer was used below 0.6 eV, and the grating monochromators were used for 0.5–20 eV.¹² The reflectivity spectra above 5 eV were measured at the Normal Incident Monochromator beamline in Pohang Light Source. Using the liquid-He cooled cryostat, the temperature-dependent $R(\omega)$ were measured for the region of 5 meV–5 eV. After the reflectivity measurements, the gold normalization techniques were used to take into account the surface scattering effect.¹³

III. RESULTS AND DISCUSSIONS

Figure 1 shows the temperature-dependent dc resistivities $\rho(T)$ of $\text{Sr}_2(\text{Fe}_{1-z}\text{Mn}_z)\text{MoO}_6$. With change of z , large variations of $\rho(T)$ can be seen. $\rho(T)$ of $\text{Sr}_2\text{FeMoO}_6$, i.e., $z=0.0$, shows a metallic behavior ($d\rho/dT > 0$) within our measured temperature ranges. As z increases, the absolute value of $\rho(T)$ continuously increases and $\rho(T)$ shows an insulating behavior ($d\rho/dT < 0$) for $\text{Sr}_2\text{MnMoO}_6$, i.e., $z=1.0$. Such a systematic change of $\rho(T)$ can be understood by the change of charge-carrier number in the Mo 4d band, and the metal–insulator transition seemed to occur around $z \approx 0.2$.

The ferrimagnetic ordering temperature T_c also systematically decreases with increasing z , denoted by the arrows. T_c of $z=0.0$ is estimated around 400 K. As z increases, T_c con-

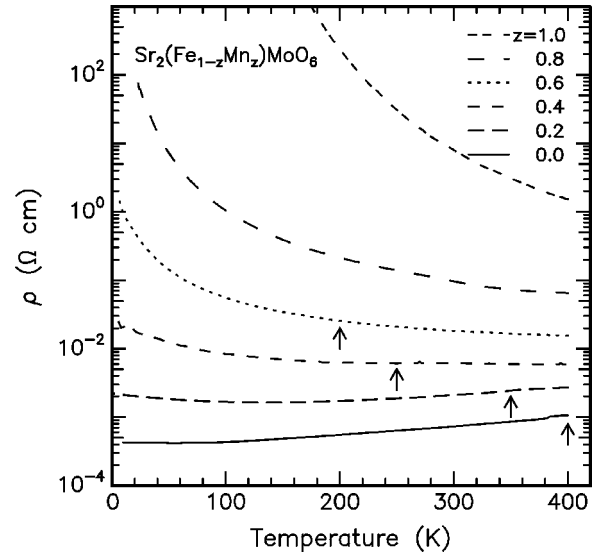


FIG. 1. Temperature-dependent dc resistivities of $\text{Sr}_2(\text{Fe}_{1-z}\text{Mn}_z)\text{MoO}_6$. The arrows represent the ferrimagnetic ordering temperatures.

tinuously decreases and disappears above $z > 0.6$. Note that there should be a correlation between $\rho(T)$ and T_c . The value of T_c decreases as that of $\rho(T)$ increases. This might suggest that the Mo 4d charge-carriers mediate the magnetic ordering of the local spins.

Figure 2 shows the doping-dependent $R(\omega)$ of the $\text{Sr}_2(\text{Fe}_{1-z}\text{Mn}_z)\text{MoO}_6$ single crystals at 10 K in the range 0.01–20 eV. [Since there was little change in $R(\omega)$ between 10 and 290 K near 5 eV, we smoothly connected the room temperature $R(\omega)$ above 5 eV.] In the far-infrared region, several peaks due to the optic phonon modes can be seen for

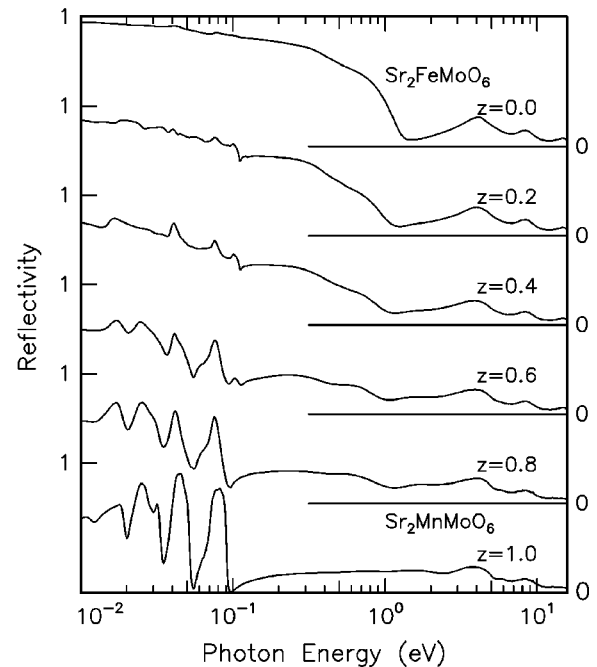


FIG. 2. Doping-dependent reflectivity spectra of $\text{Sr}_2(\text{Fe}_{1-z}\text{Mn}_z)\text{MoO}_6$ at 10 K.

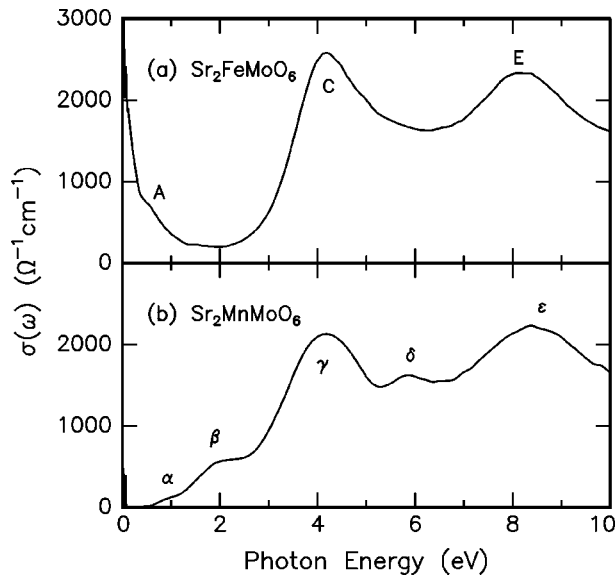


FIG. 3. $\sigma(\omega)$ of (a) $\text{Sr}_2\text{FeMoO}_6$ and (b) $\text{Sr}_2\text{MnMoO}_6$ below 10 eV. Labeled alphabet and Greek letters represent the apparent peak positions.

the insulating samples with $z > 0.2$. For the metallic samples with $z \leq 0.2$, the phonon peaks are screened and $R(\omega)$ approach 1.0 in the dc limit. In the high energy region, $R(\omega)$ are dominated by several broad peaks resulting from inter-band transitions.

Using the Kramers–Kronig transformation, optical conductivity spectra $\sigma(\omega)$ were obtained. For this analysis, $R(\omega)$ below 5 meV were extrapolated using the Hagen-Rubens relation for the metallic samples and were kept to be a constant value for the insulating samples. For the high energy region, the values of $R(\omega)$ at 20 eV were extended up to 40 eV and then ω^{-4} dependence was assumed. To check the possible errors in our Kramers–Kronig transformation, we independently measured the optical constants for the energy region of 1.5–5 eV using spectroscopic ellipsometry. The results of the Kramers-Kronig analysis agreed quite well with the ellipsometry data, confirming the validity of our transformation.

Figures 3(a) and 3(b) show $\sigma(\omega)$ of $\text{Sr}_2\text{FeMoO}_6$ and $\text{Sr}_2\text{MnMoO}_6$ at 10 K, respectively. Below 10 eV, there are several peaks originating from the optical transitions between the electronic levels. In $\text{Sr}_2\text{FeMoO}_6$, $\sigma(\omega)$ apparently show three peaks (A, C, and E) with a Drude peak at $\omega = 0$ eV. While in $\text{Sr}_2\text{MnMoO}_6$, $\sigma(\omega)$ show five peaks (α , β , γ , δ , and ϵ) with an optical gap ~ 0.5 eV. In both spectra, we can see that the peak strength is quite large above 3 eV, and the peaks (C and E) in $\text{Sr}_2\text{FeMoO}_6$ and those (γ and ϵ) in $\text{Sr}_2\text{MnMoO}_6$ are located at similar positions with comparable strengths. This suggests that those peaks should be electric dipole-allowed p – d transitions and might originate from common bands such as O $2p$ and Mo $4d$. [The contribution of $\sigma(\omega)$ from Sr bands should be located above 10 eV.¹⁴] The strengths of the peaks below 3 eV are much smaller than those above 3 eV. This suggests that the former peaks might be due to the d – d transitions, which originate

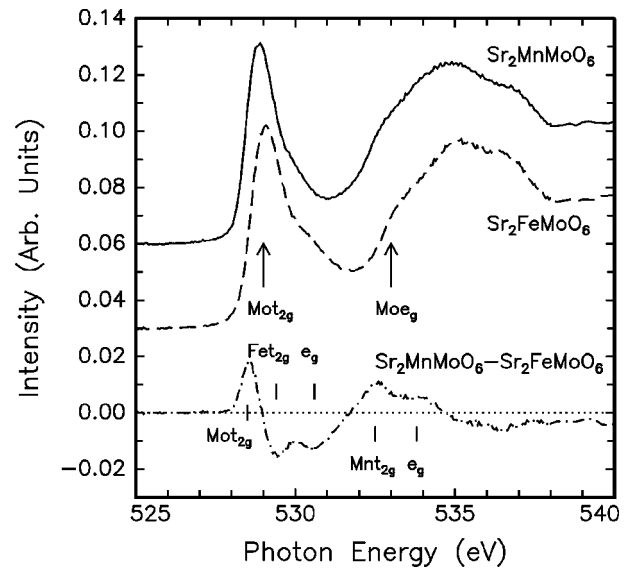


FIG. 4. O $1s$ XAS spectra of $\text{Sr}_2\text{FeMoO}_6$ (dashed line) and $\text{Sr}_2\text{MnMoO}_6$ (solid line) at 290 K. The dotted-dashed line represents the difference spectrum, which is obtained by subtracting the $\text{Sr}_2\text{FeMoO}_6$ spectrum from the $\text{Sr}_2\text{MnMoO}_6$ spectrum.

from the Mo $4d$ and Fe $3d$ bands or the Mo $4d$ and Mn $3d$ bands.

Photoemission spectroscopy and O $1s$ XAS spectra provide information on the densities of filled and empty states, respectively. On the other hand, optical spectra are proportional to densities of both initial and final states with appropriate matrix elements. Thus, it is sometimes rather difficult to identify the peak origin correctly using the optical spectra only. (However, the optical spectra can provide absolute values of the spectral weight, if the peak origins are correctly determined.) Therefore, it would be quite useful to perform optical investigation combined with other spectroscopic tools, such as the photoemission and/or O $1s$ XAS measurements.

Figure 4 shows the O $1s$ XAS spectra of $\text{Sr}_2\text{FeMoO}_6$ (dashed line) and $\text{Sr}_2\text{MnMoO}_6$ (solid line). Both spectra are dominated by the Mo $4d$ bands due to the strong covalent bonding between Mo $4d$ and O $2p$. One can locate the Mo t_{2g} and e_g bands, which are separated by the crystal field splitting energy $10 Dq$ of about 4 eV, denoted by arrows. The broad peaks around 535 eV are due to the Sr $5s/4d$ bands. Meanwhile, the Fe(Mn) $3d$ bands are not clearly shown in the spectra because their intensities are small due to the relatively weak bonding strength with O $2p$ and embedded under the dominating Mo bands. However, the Fe(Mn) bands can be more easily identified by subtracting out the Mo bands.

The dotted-dashed line in Fig. 4 shows the difference spectrum, which is obtained by subtracting the $\text{Sr}_2\text{FeMoO}_6$ spectrum from the $\text{Sr}_2\text{MnMoO}_6$ spectrum. It clearly shows one double-peak feature with a negative intensity around 530 eV and another with a positive intensity around 533 eV. The spectra of $\text{Sr}_2\text{FeMoO}_6$ and $\text{Sr}_2\text{MnMoO}_6$ contain the contributions of the Fe bands and Mn bands, respectively. Thus, the Fe t_{2g} – e_g bands appear with negative intensity, while the

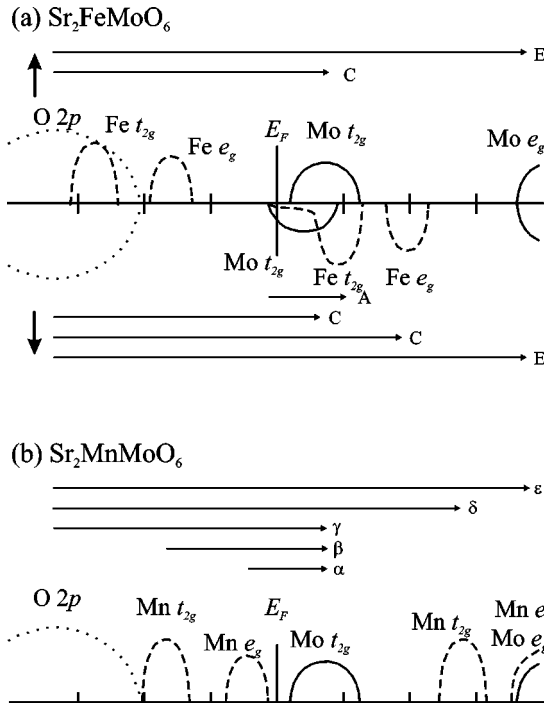


FIG. 5. Schematic diagrams of electronic band structures for (a) $\text{Sr}_2\text{FeMoO}_6$ and (b) $\text{Sr}_2\text{MnMoO}_6$. For clarity, we represent the Mo, Fe(Mn), and O bands as the solid, dashed, and dotted lines, respectively.

$\text{Mn } t_{2g}-e_g$ bands appear with positive intensity. Note that the Fe $3d$ bands are lower by ~ 3 eV compared to the Mn $3d$ bands. This energy difference can be understood by the difference between O $2p$ to Fe $3d$ and O $2p$ to Mn $3d$ charge transfer energies.¹⁵ The crystal field splitting energy, $10 Dq$, is estimated to be 1.1 ± 0.1 eV and 1.3 ± 0.1 eV for the Fe and Mn $3d$ bands, respectively. The difference spectra also show a sharp peak at the O $1s$ absorption threshold, which should be due to the chemical potential shift induced by the substitution of Fe with Mn. In $\text{Sr}_2\text{FeMoO}_6$, the chemical potential is located at the $\text{Mo } t_{2g}\downarrow$ band, which is partially occupied. When Fe is substituted with Mn, the chemical potential gradually shifts down, and it becomes located below the $\text{Mo } t_{2g}$ band in $\text{Sr}_2\text{MnMoO}_6$ so that the $\text{Mo } t_{2g}$ band is fully unoccupied. Such a gradual shift of the chemical potential was confirmed in the O $1s$ XAS spectra of $\text{Sr}_2(\text{Fe}_{1-z}\text{Mn}_z)\text{MoO}_6$ for different z values,¹⁶ and the energy shift of the O $1s$ XAS threshold was obtained as ~ 0.2 eV for $z = 0.0$ and $z = 1.0$.

Based on the valence band photoemission spectra of $\text{Ba}_2\text{FeMoO}_6$ (Ref. 17) and the O $1s$ XAS spectra in Fig. 4, we determine schematic diagrams of the electronic band structures for the end members. Figures 5(a) and 5(b) display the schematic diagrams for $\text{Sr}_2\text{FeMoO}_6$ and $\text{Sr}_2\text{MnMoO}_6$, respectively.

As shown in Fig. 5(a), the electronic structure of $\text{Sr}_2\text{FeMoO}_6$ should be split into the majority spin (up-spin) and minority spin (down-spin) bands due to the half-metallicity. The $\text{Mo } t_{2g}\downarrow$ and $\text{Fe } t_{2g}\downarrow$ bands cross the Fermi level E_F for the minority spin, while there is a gap between

$\text{Fe } e_g\uparrow$ and $\text{Mo } t_{2g}\uparrow$ bands for the majority spin. The occupied $\text{Fe } t_{2g}\uparrow$ and $\text{Fe } e_g\uparrow$ bands are located around 3 and 1.5 eV below E_F , respectively, consistent with the recent photoemission results for $\text{Ba}_2\text{FeMoO}_6$.¹⁷

As shown in Fig. 5(b), there is no electronic band splitting of $\text{Sr}_2\text{MnMoO}_6$ since it does not have the half-metallic state. Since the valence band structures are not reported yet, the valence band energy diagram could be rather difficult to be assigned. However, we can assign each levels based on the following reasons. First, the crystal structures are nearly the same for both compounds, and the Mo and O are common, so we can regard the O $2p$ and Mo $4d$ bands as nearly the same as those of $\text{Sr}_2\text{FeMoO}_6$, as confirmed in Figs. 3 and 4. Second, the crystal field splitting energies are similar, as confirmed in Fig. 4, and the Coulomb repulsion energies are also similar for Fe and Mn, the energy differences between filled and unfilled levels should be also similar. Therefore, the energy levels of the filled Fe bands, i.e., $\text{Fe } t_{2g}$ and $\text{Fe } e_g$, are lower than those of Mn bands, i.e., $\text{Mn } t_{2g}$ and $\text{Mn } e_g$. Note that these schematic diagrams turn out to be similar to recent LSDA+U band calculation results for both compounds.¹⁸

Based on above schematic band diagrams, we can assign the origins of each peak in Figs. 3(a) and 3(b). In $\text{Sr}_2\text{MnMoO}_6$, the peaks γ , δ , and ϵ can be assigned as the O $2p \rightarrow \text{Mo } t_{2g}$, O $2p \rightarrow \text{Mn } t_{2g}$, and O $2p \rightarrow \text{Mn } e_g$ ($\text{Mo } e_g$) transitions, respectively. These peaks have characteristics of dipole-allowed $p-d$ transitions, so they have large peak strengths. The two small peaks α and β can be assigned as the $\text{Mn } e_g \rightarrow \text{Mo } t_{2g}$ and $\text{Mn } t_{2g} \rightarrow \text{Mo } t_{2g}$ transitions, respectively. The strength of the α peak is quite small, since it is a $d-d$ transition between the $\text{Mn } e_g$ and $\text{Mo } t_{2g}$ bands. The energy differences ~ 4 eV between γ and ϵ , and ~ 1.2 eV between α and β represent the crystal field splitting energy of Mo $4d$ and Mn $3d$, respectively, as observed in the O $1s$ XAS spectrum.

In $\text{Sr}_2\text{FeMoO}_6$, the peaks C and E can be assigned as the O $2p \rightarrow \text{Mo } t_{2g}$ ($\text{Fe } t_{2g}$, $\text{Fe } e_g$) and O $2p \rightarrow \text{Mo } e_g$ transitions, respectively. Note that, in $\text{Sr}_2\text{MnMoO}_6$, the peaks originating from O $2p \rightarrow \text{Mo } t_{2g}$ and O $2p \rightarrow \text{Mn } t_{2g}$ are well separated, however, in $\text{Sr}_2\text{FeMoO}_6$, the peaks from O $2p \rightarrow \text{Mo } t_{2g}$ and O $2p \rightarrow \text{Fe } t_{2g}$ (also, O $2p \rightarrow \text{Fe } e_g$) are not well separated due to the very close energy positions of $\text{Mo } t_{2g}$ and $\text{Fe } t_{2g}$ ($\text{Fe } e_g$) bands. In fact, the peak of C is somewhat broader than that of γ , and the strength of C is larger than that of γ . The peak corresponding to β for $\text{Sr}_2\text{FeMoO}_6$, i.e., $\text{Fe } t_{2g} \rightarrow \text{Mo } t_{2g}$, should be located above 3 eV, and thus there is no clear peak-like structure near 2 eV. The peak corresponding to α for $\text{Sr}_2\text{FeMoO}_6$, i.e., $\text{Fe } e_g \rightarrow \text{Mo } t_{2g}$ should be located above 1 eV. [The $\text{Fe } t_{2g} \rightarrow \text{Mo } t_{2g}$ and $\text{Fe } e_g \rightarrow \text{Mo } t_{2g}$ transitions are not clearly appeared in Fig. 3(a) due to the large and broad background of peak C.] The peak A can be assigned as the $\text{Mo } t_{2g} \rightarrow \text{Fe } t_{2g}$ transition through the down-spin channel.

The peak A was assigned by some workers as the $\text{Fe } e_g\uparrow \rightarrow \text{Mo } t_{2g}\uparrow$ transition with the assumption that the $\text{Mo } t_{2g}\downarrow$ and $\text{Fe } t_{2g}\downarrow$ bands were nearly degenerated.⁹ However, if the peak A originates from the $\text{Fe } e_g\uparrow \rightarrow \text{Mo } t_{2g}\uparrow$ transition, the peak strength A should be comparable to that of α in

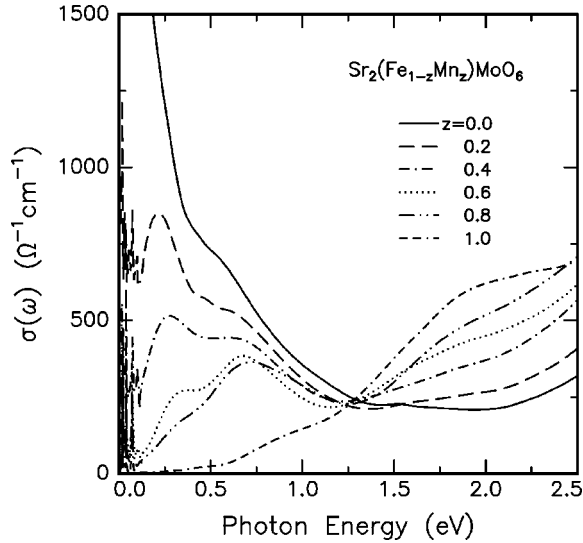


FIG. 6. Doping-dependent $\sigma(\omega)$ of $\text{Sr}_2(\text{Fe}_{1-z}\text{Mn}_z)\text{MoO}_6$ at 10 K.

$\text{Sr}_2\text{MnMoO}_6$. In addition, the peak A should be located at a higher energy than α . Therefore, our assignment of peak A as the $\text{Mo } t_{2g}\downarrow \rightarrow \text{Fe } t_{2g}\downarrow$ is more reasonable and such an assignment can explain the doping dependent $\sigma(\omega)$, as shown later. Also, recent LSDA+U calculation result clearly shows that the $\text{Mo } t_{2g}\downarrow$ and $\text{Fe } t_{2g}\downarrow$ bands are separated, since the U values are different for the Fe and Mo ions.¹⁹

To understand the changes of electronic structure from the metallic $\text{Sr}_2\text{FeMoO}_6$ to the insulator $\text{Sr}_2\text{MnMoO}_6$, we show the doping (z)-dependent $\sigma(\omega)$ below 2.5 eV in Fig. 6. For the $z = 1.0$ sample, there are two peaks α (centered around 0.8 eV) and β (centered around 2.0 eV) with the optical gap ~ 0.5 eV. As the number of Mo 4d charge-carriers increases (i.e., as z decreases), the high energy spectral weight decreases and the low energy spectral weight increases. Based on our schematic diagrams of Figs. 5(a), and 5(b), we can regard that the peaks of α and β shift to higher energy with decreasing z . Then, the continuous decrease of high energy peak strength can be understood. In the low energy region, the spectral weight increases due to the increase of the occupation of $\text{Mo } t_{2g}\downarrow$ and $\text{Fe } t_{2g}\downarrow$ bands. Finally in metal, $z = 0.0$, there is the Drude peak and the broad peak A, which was also observed by Tomioka *et al.*⁹

The Mo 4d charge-carriers do not form the Drude peak for most doping ranges, i.e., $0.2 \leq z \leq 0.8$, but turn into the Drude peak for the $z = 0.0$ sample. The plasma frequency ω_p of $z = 0.0$ is estimated using the relation of $\frac{1}{8}\omega_p^2 = \int_0^\infty \sigma_d(\omega') d\omega'$, where $\sigma_d(\omega)$ is the Drude peak, giving value of $\omega_p \sim 1.8$ eV. Note that the value of 1.8 eV is small when we compare with the same quantity calculated from the free electron mass and the known value of carrier number $n = 1.1 \times 10^{22}/\text{cm}^3$ (Ref. 9). This result might suggest the correlation effect of Mo carriers in double perovskites. (In fact, the effective mass is reported to be larger than the free electron mass by recent specific heat measurements.¹⁹) A degree of site disorder of Fe ions at Mo sites and/or Mo ions at Fe sites, however, can be the main source for localization of the

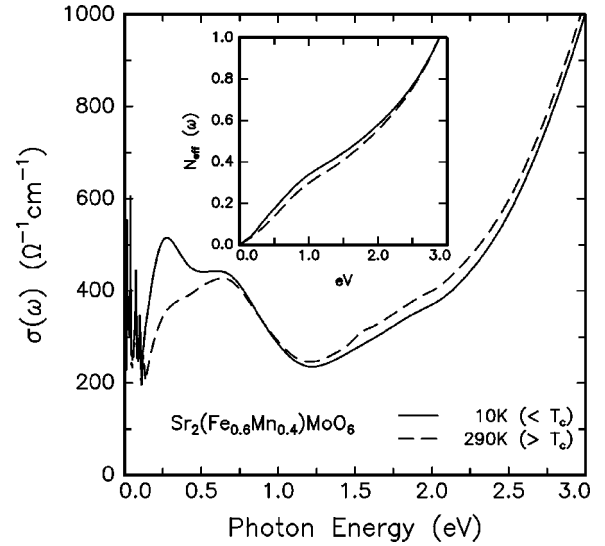


FIG. 7. Temperature-dependent $\sigma(\omega)$ of $\text{Sr}_2(\text{Fe}_{0.6}\text{Mn}_{0.4})\text{MoO}_6$ at 290 K ($>T_c$) and 10 K ($<T_c$). The inset shows the $N_{\text{eff}}(\omega)$ which is obtained by integrating $\sigma(\omega)$.

charge-carriers in double perovskites. It has been known that site disorder, which strongly depends on the sample preparation method,²⁰ plays a crucial role in some physical properties, such as low-field magnetoresistance.²¹ Even for our $\text{Sr}_2(\text{Fe}_{1-z}\text{Mn}_z)\text{MoO}_6$ single crystalline samples, there should be a certain degree of site disorder and it will effect $\sigma(\omega)$.²² For example, the free carrier motions through the Fe–Mo–Fe chains or Mo–Mo chains²³ will be disturbed; hence the low energy peak can be formed rather than the Drude peak for $0.2 \leq z \leq 0.8$ and the Drude peak for the $z = 0.0$ sample becomes small. The issues of correlation and site disorder effects on $\sigma(\omega)$ of double perovskites require further systematic studies.

To understand the electronic structure changes with ferrimagnetic spin ordering in double perovskites, we also investigated $\sigma(\omega)$ of $\text{Sr}_2(\text{Fe}_{0.6}\text{Mn}_{0.4})\text{MoO}_6$ ($T_c \sim 250$ K) at 290 K ($>T_c$) and 10 K ($<T_c$), as shown in Fig. 7. For $\text{Sr}_2\text{FeMoO}_6$ ($T_c \sim 400$ K), we attempted reflectivity measurements at 500 K. However, after the high temperature measurements, we found that the color of the surface became changed, possibly due to the change in oxygen stoichiometry. So, we could not investigate $\sigma(\omega)$ of $z = 0.0$ above T_c . The temperature-dependent behaviors of $\sigma(\omega)$ for $z = 0.0$ from 290 to 10 K were found to be similar to those for $z = 0.4$ from above to below T_c . For $z = 1.0$, there was no considerable variation in $\sigma(\omega)$ between 290 and 10 K.

With the ferrimagnetic ordering, $\sigma(\omega)$ are changed for a wide energy region below 3 eV. The spectral weight above 1.0 eV is transferred to the low energy region below 1.0 eV.²⁴ Since the change of $\sigma(\omega)$ in the high energy region is rather small and broad, we have measured $R(\omega)$ several times, and found that the changes in $\sigma(\omega)$ were quite reproducible. We estimated the effective number of carriers, $N_{\text{eff}}(\omega)$, using $N_{\text{eff}}(\omega) = (2m_e V / \pi e^2) \int_0^\omega \sigma(\omega') d\omega'$, where m_e and V represent the free electron mass and unit-cell volume, respectively. When we integrate $\sigma(\omega)$ up to 3 eV, as shown in the inset, $N_{\text{eff}}(\omega)$ is nearly the same for above and below T_c ,

indicating that the optical sum rule becomes satisfied within the spectral region below 3 eV. This result suggests that there is a redistribution of the spectral weight in the energy region upon cooling through T_c .

It might be considered that the spectral weight changes of double perovskites are quite similar to those of manganites.²⁵ In manganites, the spin-split band model based on the double-exchange mechanism²⁶ has explained such spectral weight transfer. Above T_c , $\sigma(\omega)$ show a peak due to the interband transition between the Hund's rule split bands such as $\text{Mn } e_g \uparrow [\text{Mn} t_{2g} \uparrow] \rightarrow \text{Mn } e_g \uparrow [\text{Mn} t_{2g} \downarrow]$. (This notation indicates that the transitions occur between two e_g bands with the same spin but different t_{2g} spin background.) Below T_c , the background spins of the Mn t_{2g} ions become aligned and the interband transition will be prohibited, and the spectral weight will move to the low energy Drude-like absorption.

If such spin-split band model is applicable for double perovskites, the Hund's rule splitting of the Mo ions should be quite large to explain such large energy scale (i.e., ~ 3 eV) change in $\sigma(\omega)$. Generally, the Mo ion is nonmagnetic, so the Hund's rule exchange energy is considered to be much smaller than that of the Mn ion. However, Sarma *et al.*²⁷ recently proposed the unusual renormalization of the intra-atomic exchange strength at the Mo ions (0.8–1.5 eV) arising from the Fe–Mo interaction. Although this scenario is quite interesting, as far as we know, there is little experimental data to support this scenario. In manganites, the bandwidth of Mn e_g is known to be smaller than the Hund's exchange energy, so that the Hund's rule split band model could be applicable. However, in double perovskites, the bandwidth of Mo is expected to be larger than the band splitting between Mo $t_{2g} \uparrow$ and Mo $t_{2g} \downarrow$. Moreover, our O 1s spectra of $\text{Sr}_2\text{FeMoO}_6$ are similar to those of $\text{Sr}_2\text{MnMoO}_6$, as shown in Fig. 4. This suggests that the spin-split band model for the Mo ion might be not sufficient to explain the spectral weight change with ferrimagnetic ordering in the double perovskites.

The increase of the spectral weight in low energy region can be explained by the increase of hopping motion of charge carriers. Once the Fe t_{2g} spins are ferromagnetically aligned, the aligned Mo $t_{2g} \downarrow$ electrons easily move to the Fe $t_{2g} \downarrow$ sites to yield a kinetic energy gain. Note that many reports have suggested that the Fe ions have intermediate valence states between Fe^{2+} and Fe^{3+} .²⁸ Then, there should be a finite number of Fe $t_{2g} \downarrow$ electrons. The increased low

energy spectral weight should come from the decreased spectral weight in the high energy region. The origin of decreased spectral weight in the high energy region is not so clear at the current stage, since it occurs near the tail of broad and strong charge transfer peaks. However, our observation that the sum rule is satisfied by integrating up to 3 eV with ferrimagnetic ordering suggests that the Mo band should be hybridized with the Fe band and the corresponding spectral weight become redistributed due to the Fe spin ordering.²⁹

IV. SUMMARY

We investigated electronic structure changes induced by the filling control of the Mo 4d charge-carriers in double perovskite $\text{Sr}_2(\text{Fe}_{1-z}\text{Mn}_z)\text{MoO}_6$ using optical conductivity measurements. With doping, we observed large spectral weight changes in a wide photon energy region. Using the detailed analyses of optical conductivity spectra and O 1s x-ray absorption spectroscopy results, we found that such changes should originate from the fact that the energy levels of the Fe 3d and Mn 3d bands are located at quite different positions. Below the gap of $\text{Sr}_2\text{MnMoO}_6$ (~ 0.5 eV), the in-gap states start to appear with doping and finally the Drude peak appears in $\text{Sr}_2\text{FeMoO}_6$. The strength of the in-gap state increases with the increase of the Mo 4d charge-carriers, but it does not form a Drude peak above $z \geq 0.2$, which is probably due to the site disorder effects. We have also observed the spectral weight transfer from high to low energy region with the ferrimagnetic ordering. The spectral changes occur over a rather wide energy scale of ~ 3 eV, suggesting the redistribution of electronic structure due to the Mo–Fe hybridization.

ACKNOWLEDGMENTS

We acknowledge Professors Jaejun Yu, K. T. Park, and J.-S. Kang for helpful discussions. This work was supported by the Ministry of Science and Technology through the Creative Research Initiative Program, and by the Korea Science and Engineering Foundation through the CSCMR at Seoul National University, and also by Kurata Foundation, Japan. The work at POSTECH was supported by KOSEF through the eSSC at POSTECH, and BK 21 project of Ministry of Education, Korea. Experiments at PLS were supported in part by MOST and POSCO.

¹S. Jin, T.H. Tiefel, M. McCormack, R.A. Fastnacht, R. Ramesh, and L.H. Chen, *Science* **264**, 413 (1994).

²K.-I. Kobayashi, T. Kimura, H. Sawada, K. Terakura, and Y. Tokura, *Nature (London)* **395**, 677 (1998); K.-I. Koyahashi, T. Kimura, Y. Tomioka, H. Sawada, K. Terakura, and Y. Tokura, *Phys. Rev. B* **59**, 11 159 (1999).

³T.H. Kim, M. Uehara, S-W. Cheong, and S. Lee, *Appl. Phys. Lett.* **74**, 1737 (1999); B-G. Kim, Y-S. Hor, and S-W. Cheong, *ibid.* **79**, 388 (2001).

⁴T. Kise, T. Ogasawara, M. Ashida, Y. Tomioka, Y. Tokura, and M.

Kuwata-Gonokami, *Phys. Rev. Lett.* **85**, 1986 (2000).

⁵S. Ray, A. Kumar, D.D. Sarma, R. Cimino, S. Turchini, S. Zennaro, and N. Zema, *Phys. Rev. Lett.* **87**, 097204 (2001).

⁶M. Itoh, I. Ohota, and Y. Inaguma, *Mater. Sci. Eng., B* **41**, 55 (1996).

⁷Y. Okimoto, T. Katsufuji, T. Ishikawa, A. Urushibara, T. Arima, and Y. Tokura, *Phys. Rev. Lett.* **75**, 109 (1995); S.G. Kaplan, M. Quijada, H.D. Drew, D.B. Tanner, G.C. Xiong, R. Ramesh, C. Kwon, and T. Venkatesan, *ibid.* **77**, 2081 (1996); K.H. Kim, J.Y. Gu, H.S. Choi, G.W. Park, and T.W. Noh, *ibid.* **77**, 1877 (1996);

- K.H. Kim, J.H. Jung, and T.W. Noh, *ibid.* **81**, 1517 (1998); H.L. Liu, S.L. Cooper, and S-W. Cheong, *ibid.* **81**, 4684 (1998).
- ⁸Y. Moritomo, Sh. Xu, A. Machida, T. Akimoto, E. Nishibori, M. Takata, and M. Sakata, *Phys. Rev. B* **61**, R7827 (2000).
- ⁹Y. Tomioka, T. Okuda, Y. Okimoto, R. Kumai, K.-I. Kobayashi, and Y. Tokura, *Phys. Rev. B* **61**, 422 (2000).
- ¹⁰Y. Moritomo, H. Kusuya, A. Machida, E. Nishibori, M. Takata, M. Sakata, and A. Nakamura, *J. Phys. Soc. Jpn.* **70**, 3182 (2001); Y. Moritomo, N. Shimamoto, S. Xu, A. Machida, E. Nishibori, M. Takata, M. Sakata, and A. Nakamura, *Jpn. J. Appl. Phys., Part 2* **40**, L672 (2001).
- ¹¹F.M.F. de Groot, M. Grioni, J.C. Fuggle, J. Ghijsen, G.A. Sawatzky, and H. Peterson, *Phys. Rev. B* **40**, 5715 (1989); J.-H. Park, C.T. Chen, S-W. Cheong, W. Bao, G. Meigs, V. Chakarian, and Y.U. Idzerda, *Phys. Rev. Lett.* **76**, 4215 (1996).
- ¹²J.H. Jung, K.H. Kim, D.J. Eom, T.W. Noh, E.J. Choi, J. Yu, Y.S. Kwon, and Y. Chung, *Phys. Rev. B* **55**, 15 489 (1997).
- ¹³H.J. Lee, J.H. Jung, Y.S. Lee, J.S. Ahn, T.W. Noh, K.H. Kim, and S-W. Cheong, *Phys. Rev. B* **60**, 5251 (1999).
- ¹⁴J.S. Lee, Y.S. Lee, T.W. Noh, K. Char, J. Park, S.-J. Oh, J.-H. Park, C.B. Eom, T. Takeda, and R. Kanno, *Phys. Rev. B* **64**, 245107 (2001).
- ¹⁵Similarly, the charge transfer energy of MnO was reported to be ~ 4 eV larger than that of Fe₂O₃. See A. Fujimori, M. Saeki, N. Kimizuka, M. Taniguchi, and S. Suga, *Phys. Rev. B* **34**, 7318 (1986); A. Fujimori, N. Kimizuka, T. Akahane, T. Chiba, S. Kimura, F. Minami, K. Siratori, M. Taniguchi, S. Ogawa, and S. Suga, *ibid.* **42**, 7580 (1990).
- ¹⁶J.-H. Park (unpublished).
- ¹⁷We refer the valence spectra of Ba₂FeMoO₆, since there is no data on Sr₂FeMoO₆. See, J.-S. Kang, H. Han, B.W. Lee, C.G. Olson, S.W. Han, K.H. Kim, J.I. Jeong, J.H. Park, and B.I. Min, *Phys. Rev. B* **64**, 024429 (2001).
- ¹⁸H. Wu, *Phys. Rev. B* **64**, 125126 (2001).
- ¹⁹Y. Moritomo, Sh. Xu, T. Akimoto, A. Machida, N. Hamada, K. Ohoyama, E. Nishibori, M. Takata, and M. Sakata, *Phys. Rev. B* **62**, 14 224 (2000).
- ²⁰L.I. Balcells, J. Navarro, M. Bibes, A. Roig, B. Martinez, and J. Fontacuberta, *Appl. Phys. Lett.* **78**, 781 (2001).
- ²¹M. Garcia-Hernandez, J.L. Martinez, M.J. Martinez-Lope, M.T. Casais, and J.A. Alonso, *Phys. Rev. Lett.* **86**, 2443 (2001).
- ²²In fact, we found that the phonon mode, located around 600 cm⁻¹, for 0.0 ≤ z ≤ 0.8, is quite broad. Although more systematic studies, such as disorder dependent infrared phonon mode, are needed, the large width of phonon mode (~ 80 cm⁻¹) might be related with the site-disorder in double perovskite as observed in other disordered samples [see A.S. Barker, Jr. and A.J. Sievers, *Rev. Mod. Phys.* **47**, FS1 (1975)].
- ²³There has been a report that the direct Mo *t*_{2g}-Mo *t*_{2g} interaction is a main cause of the metallic behavior. See J. Gopalakrishnan, A. Chattopadhyay, S.B. Ogale, T. Venkatesan, R.L. Greene, A.J. Millis, K. Ramesha, B. Hannoyer, and G. Marest, *Phys. Rev. B* **62**, 9538 (2000).
- ²⁴As seen in Fig. 6, the mid-infrared spectral weight could be affected by the site disorder. If there is no site disorder, we might surmise that the increase of the low energy spectral weight is realized as increase of the Drude-like component.
- ²⁵Y. Moritomo, A. Machida, K. Matsuda, M. Ichida, and A. Nakamura, *Phys. Rev. B* **56**, 5088 (1997).
- ²⁶C. Zener, *Phys. Rev.* **82**, 403 (1951); P.W. Anderson and H. Hasegawa, *ibid.* **100**, 67 (1955).
- ²⁷D.D. Sarma, P. Mahadevan, T. Saha-Dasgupta, S. Ray, and A. Kumar, *Phys. Rev. Lett.* **85**, 2549 (2000).
- ²⁸See, for example, J. Linden, T. Yamamoto, M. Karppinen, and H. Yamauchi, *Appl. Phys. Lett.* **76**, 2925 (2000).
- ²⁹Z. Fang, K. Terakura, and J. Kanamori, *Phys. Rev. B* **63**, 180407(R) (2001).